

# **Investigating the effect of phospholipids on droplet formation and surface property evolution in microfluidic devices for droplet interface bilayer (DIB) formation**

Elanna B. Stephenson, Ricardo García Ramírez, Sean Farley, Katherine Adolph-Hammond, Gihun Lee, John M. Frostad & Katherine S. Elvira

2022

Faculty of Science

Faculty Publications

This is a postprint version of the article.

The final publication is available at:

Stephenson, E. B., Ramírez, R. G., Farley, S., Adolph-Hammond, K., Lee, G., Frostad, J. M., & Elvira, K. S. (2022). Investigating the effect of phospholipids on droplet formation and surface property evolution in microfluidic devices for droplet interface bilayer (DIB) formation. *Biomicrofluidics*, 16(4).

<https://doi.org/10.1063/5.0096193>

---

Downloaded from UVicSpace Research & Learning Repository

dspace.library.uvic.ca



**University  
of Victoria**

Libraries

# Investigating the effect of phospholipids on droplet formation and surface property evolution in microfluidic devices for droplet interface bilayer (DIB) formation

Elanna B. Stephenson,<sup>†,‡</sup> Ricardo Garca Ramirez,<sup>¶</sup> Sean Farley,<sup>†,‡</sup> Katherine Adolph-Hammond,<sup>†</sup> Gihyun Lee,<sup>†</sup> John M. Frostad,<sup>§</sup> and Katherine S. Elvira<sup>\*,†,‡</sup>

<sup>†</sup>*Department of Chemistry, University of Victoria, Canada*

<sup>‡</sup>*Centre for Advanced Materials and Related Technology (CAMTEC), University of Victoria, Canada.*

<sup>¶</sup>*School of Engineering and Sciences, Tecnológico de Monterrey, Mexico*

<sup>§</sup>*Chemical and Biological Engineering, University of British Columbia, Canada*

<sup>||</sup>*Food Science, University of British Columbia, Canada*

E-mail: kelvira@uvic.ca

## Abstract

Despite growing interest in droplet microfluidic methods for droplet interface bilayer (DIB) formation, there is a dearth of information regarding how phospholipids impact device function. Limited characterisation has been carried out for phospholipids, either computationally *in silico* or experimentally *in situ* in PDMS microfluidic devices, despite recent work providing a better understanding of how other surfactants behave in microfluidic systems. Hence, microfluidic device design for DIB applications

therefore relies heavily on trial and error, with many assumptions made about the impact of phospholipids on droplet formation and surface properties. Here we examine the effects of phospholipids on interfacial tension, droplet formation, wetting and hence device longevity using DPhPC as the most widely used lipid for DIB formation. We use a customised COMSOL *in silico* model in comparison with *in situ* experimental data to establish that the stabilisation of droplet formation seen when the lipid is dosed in the aqueous phase (lipid-in) or in the oil phase (lipid-out) is directly dependent on the effects of lipids on the device surface properties, rather than how fast they coat the droplet. Furthermore, we establish a means to visually characterise surface property evolution in the presence of lipids, and explore rates of device failure in the absence of lipid, lipid-out, and lipid-in. This first exploration of the effects of lipids on device function may serve to inform the design of microfluidic devices for DIB formation, as well as to troubleshoot causes of device failure during microfluidic DIB experiments.

## Introduction

Droplet interface bilayers (DIBs) are artificial membranes that are increasingly being used as an easily customisable model of cellular structures and processes, most recently for drug discovery applications.<sup>1,2</sup> The artificial cell bilayer in DIBs is created at the interface between two monolayer covered droplets, which are usually suspended in an oil phase. Microfluidic technologies are commonly used to create and control these systems. When making droplets for DIB creation on a microfluidic device, it is necessary to form aqueous droplets within an oil carrier phase and hence surface (or interface) physics plays a critical role in this process.<sup>3</sup> Despite the growing interest in using microfluidic devices to form DIBs,<sup>2</sup> the behaviour of phospholipids as surfactants in microfluidic devices has been largely overlooked, and any interaction that they have with surfaces in a microfluidic device remains unstudied and poorly understood. This affects research in the field in two main ways. Firstly, it limits our ability to mitigate detrimental effects associated with surface interactions in the microfluidic de-

vice, hence reducing device lifetime and potentially restricting the types of lipids (and other molecules) used for DIB formation. And secondly, we are not able to determine whether the device itself is affecting the distribution of lipids in the aqueous system, and hence the composition of the artificial bilayer.

Microfluidic devices are commonly made from the polymer polydimethylsiloxane (PDMS). PDMS has numerous advantages when being used for droplet microfluidic devices. The natural hydrophobicity of PDMS in theory serves to assist in the formation of aqueous droplets in an oil phase.<sup>?</sup> In practice however, PDMS is a complex material which can present considerable challenges when used for droplet microfluidics. PDMS is gas permeable<sup>?</sup> and permeable to oils such as hexadecane and squalene,<sup>?</sup> which cause evaporation of aqueous droplets and swelling of the device geometry respectively. In cases where adsorption of surfactants to the walls of the device is critical for stable droplet formation, excessive contact with water may lead to device failure by removal of the adsorbed surfactant.<sup>?</sup> <sup>?</sup> The permeable, flexible nature of PDMS furthermore complicates permanent surface modification, as high surface energy chains present at the surface will become internalized within the PDMS structure as the surface moves and shifts, a process called reconstruction.<sup>?</sup>

Because fluid and surface properties have such a profound effect on the process of droplet formation, the use of surfactants (or emulsifiers) is common within the field of droplet microfluidics, and in some cases they are critical to the operation of a device by stabilising emulsions or reducing interfacial tension at droplet-generating, on-chip geometries.<sup>?</sup> When making DIBs, phospholipids also act as the surfactant for the oil/water system.<sup>?</sup> This is because formation of a DIB depends both upon the amphiphilic nature of phospholipids, where hydrophilic headgroups and hydrophobic tails cause specific arrangement of the molecules when in solution, and on their emulsion stabilising properties. While phospholipids behave as a surfactant in the process of DIB formation, the kinetics of monolayer formation for both lipid-out (where lipids are dosed in the oil phase) and lipid-in (where lipids are dosed in the aqueous phase) systems suggest that in some cases they do not have time to assemble at the

oil/water interface during the relatively fast process of droplet formation.<sup>?</sup>

This phenomenon is referred to as dynamic surface tension, which is the process by which the interfacial tension decreases as surfactant migrates to the fluid interface and can often be slower than the rate of droplet formation.<sup>?</sup> Indeed, microfluidic devices for DIB formation frequently employ structural features such as meanders or switchbacks to increase the distance between the droplet generator and the point of droplet contact to ensure complete monolayer formation and reliable emulsion stabilisation.<sup>???</sup> The kinetics of this process have been established for bulk solutions via the pendant drop method,<sup>??</sup> where it has been shown that the kinetics of adsorption are dependent on the length of the droplet and can be an order of magnitude faster in microfluidic devices.<sup>??</sup> However there is limited research regarding the surfactant-like behaviour of lipids within microfluidic devices during DIB formation.

Given the unique environment present on a microfluidic device and the effect it has on surfactant assembly at fluid interfaces,<sup>?</sup> a complete picture of phospholipid behavior on microfluidic devices cannot be extrapolated from existing data. In one case, naturally derived soy lecithin has been compared to the surfactants sorbitan monooleate (Span 80) and polyglycerol polyricinoleate (PGPR) for its effect on the size of aqueous droplets created at a Y-junction and at a T-junction.<sup>?</sup> But there was no further exploration apart from noting the poor performance of lecithin compared to Span 80 and PGPR at promoting droplet formation. More recently, DIB arrays were built by exchanging the surfactant coating the droplets (Span 80) for a lipid (phosphatidylcholine, PC). This allowed the authors to determine that the relaxation time of PC was slower than for the more commonly used surfactant for droplet formation, Span 80.

While not generally discussed in the literature, it has been our experience that phospholipids frequently present challenges to reliability and longevity for microfluidic devices made from PDMS. Over time, the aqueous phase may begin to wet the walls of the device, leading to erratic droplet formation where the aqueous phase sticks to the walls of the chan-

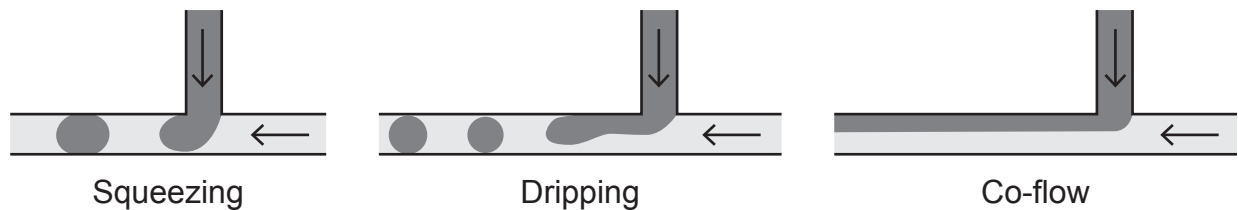


Figure 1: **Operation and failure modes of a T-junction.** Dark grey represents the aqueous phase, and light grey represents the oil phase. Arrows indicate the direction of flow. In the squeezing mode of droplet formation, shear forces cause a clean separation of the droplet at the T-junction without sticking to the walls of the device. In the dripping failure mode, the aqueous phase wets the wall of the device for a length of the main channel before droplets drip off further down the channel. In the co-flow failure mode, shear forces are unable to overcome the surface tension and wetting effects, and the two phases flow alongside each other with no droplet formation occurring.

nel and does not cleanly separate into droplets. Two of the failure modes we often see are shown in Figure 1, with one referred to as “dripping”, and the other referred to as “co-flow”. Normally the shear forces present at a T-junction lead to a clean separation of a droplet from the aqueous phase without sticking to the wall, and this intended behaviour is referred to as “squeezing”.<sup>??</sup> While laminar flow regimes predominate and the behaviour of fluids becomes more predictable at microfluidic scales, the wetting properties of the fluids on the walls of the device and the interaction at the interfaces between fluids have profound effects on how droplets behave.<sup>??</sup> Wetting refers to how a liquid interacts with a solid surface and a surface is “wetted” if the liquid sticks to the surface.<sup>?</sup> Surface modification is commonly used to change the wetting characteristics of the walls of microfluidic devices to make it more hydrophobic or hydrophilic,<sup>?</sup> but this technique is not generally required to support water-in-oil droplet formation for DIB creation unless the surfaces are not hydrophobic enough because of the material they are made from.<sup>??</sup>

The dripping failure mode serves as the primary motivation for this work. Here, for the first time we have examined the process of droplet formation for phospholipid containing solutions on a microfluidic device. The factors affecting droplet formation can be difficult to study experimentally (*in situ*), as the physical properties of the system can be difficult to

control with high precision. Hence, we are also using computational fluid dynamics (CFD) to investigate the process of droplet formation. In CFD, the Navier-Stokes equations, a set of partial differential equations describing fluid flow, are solved computationally (*in silico*). Commonly, the finite element method<sup>?</sup> is employed for this purpose, where geometry describing the system to be studied is broken down into a finite set of points, referred to as a mesh, in which to solve the equations numerically. COMSOL Multiphysics is a general-purpose physics software which can model two-phase fluid flow in both two and three dimensional space. When supplemented with data describing the physical properties of fluids obtained experimentally, as we do here, two phase CFD with software like COMSOL provides a reliable approximation of the droplet formation behaviour observed on a real microfluidic device, and has been widely employed for this purpose.<sup>?????</sup>

Here we use solutions containing the phospholipid DPhPC, which is the most commonly used lipid for DIB formation, to form droplets with both lipid-in and lipid-out configurations using the standard methods with which DIBs are usually made in microfluidic devices. This work provides insight into the process of droplet formation and experimental evidence for the adsorption of phospholipids to the walls of the device when dissolved lipid-in.

## Materials and methods

All reagents were purchased from Millipore Sigma unless otherwise stated. 1,2-diphytanoyl-*sn*-glycero-3-phosphocholine (DPhPC,  $\geq 99\%$  pure) was purchased from Avanti Polar Lipids. Polydimethylsiloxane (PDMS, Dow Sylgard 184) was purchased from Ellsworth Adhesives. Silicon wafers (100 mm diameter) were purchased from Silicon Materials. SU-8 3050 photoresist and developer were purchased from MicroChem. Polytetrafluoroethylene (PTFE) tubing (1/16" outer diameter, 250  $\mu\text{m}$  inner diameter) was purchased from Chromatographic Specialties.

## Lipid solution preparation

Lipid solutions were prepared as is usually done for DIB formation in microfluidic devices. Solutions of  $10 \text{ mg mL}^{-1}$  DPhPC in either hexadecane or aqueous buffer (10 mM HEPES pH = 7.6, 200 mM KCl) were prepared as described previously from a  $25 \text{ mg mL}^{-1}$  stock solution of DPhPC in chloroform.<sup>?</sup> In brief, stock solution was dispensed into a roundbottom flask and the solvent was removed under a stream of nitrogen before being placed under vacuum for 1 h. Lipids were then resuspended by adding hexadecane or buffer and vortexing for 3 min at room temperature. Aqueous solutions were subsequently extruded by passing through a  $0.1 \mu\text{m}$  polycarbonate membrane 21 times. We chose a concentration of DPhPC that is 3-4 orders of magnitude higher than the critical micelle concentration of DPhPC,<sup>?</sup> and 5 times higher than concentrations capable of forming DIBs in high-throughput<sup>?</sup> to ensure rapid migration of the lipid to the fluid interface.

## Microfluidic device fabrication and use

Microfluidic devices and flat surfaces (used for determining contact angles) were fabricated from PDMS as described previously.<sup>?</sup> In brief, standard photolithography methods were used to prepare an SU-8 on silicon master with a height of  $53 \pm 1 \mu\text{m}$ . PDMS was cast on either the master or a blank silicon wafer (for flat surfaces) using standard soft lithography methods, namely mixing as per the manufacturer's instructions, pouring over the wafer, degassing and then curing overnight at  $65^\circ\text{C}$ . Devices were prepared by cutting, punching access holes with a biopsy punch, and then plasma bonding to a PDMS coated glass slide. The device design was the same as described in our previous work,<sup>?</sup> but access ports were punched following the meander section so as to only use the T-junction for droplet creation.

Microfluidic experiments were carried out by mounting the devices on the stage of a Nikon Eclipse Ti2-U inverted microscope. Hexadecane and buffer solutions were dispensed from 1 mL and 100  $\mu\text{L}$  Hamilton gastight syringes respectively on a CETONI neMESYS 290N syringe pump. Fluids were dispensed through lengths of PTFE tubing attached to the

syringes by 30 gauge blunt luer lock needle tips. Images and videos were captured using a Phantom VEO 710L high speed camera.

## **Contact angle measurements**

Contact angle measurements were carried out on a Holmarc contact angle meter (H0-CAM-0B1) using the static sessile drop method.<sup>?</sup> In this method, a drop of the solution is placed on the flat surface using a needle. A camera is then used to capture an image of the droplet from the side, and the angle of the tangent line where the droplet contacts the surface is measured. Measurements were carried out in air on a flat PDMS surface.

## **Interfacial tension measurements**

Interfacial tension measurements were carried out either on a DataPhysics TBU90E goniometer, or a custom built instrument with an inverted needle for liquid/liquid measurements using the pendant drop method.<sup>?</sup> In the pendant drop method, a fluid is ejected from a needle as far as it can go before it breaks off. A photo of the suspended droplet is taken from the side. The interfacial tension is then determined by fitting a curve to the profile of the droplet, and mathematically determining the forces inducing that shape, which are an equilibrium between buoyancy and the interfacial tension. In all cases, droplets were allowed to equilibrate for 5 min before measurement to allow full monolayer formation. Images from the TBU90E goniometer were processed using OpenDrop 3.3.0,<sup>?</sup> and images acquired using the custom instrument were processed using a custom MATLAB program.

## ***In silico* fluid dynamics simulations with COMSOL**

The computational model was developed in COMSOL Multiphysics 5.6 with the Microfluidics Module on a 64-bit Windows 10 workstation. Our computational method uses an optimised model for droplet creation at a T-junction provided in the COMSOL software package.<sup>?</sup> This

Table 1: **Interfacial tension values used in the COMSOL model.** Interfacial tensions were determined between the two phases corresponding to the column and row titles. Values from literature have citations. Literature values for “buffer” refer to pure water since the salt concentrations used have negligible effect on interfacial tension. All units are  $\text{mN m}^{-1}$ .

	Air	Hexadecane	Buffer	DPhPC/hexadecane	DPhPC/buffer
Air		28.12	71.94 <sup>?</sup>	26.05	47.35
Hexadecane	28.12		55.2 <sup>?</sup>		10.89
Buffer	71.94 <sup>?</sup>	55.2 <sup>?</sup>		21.04	
DPhPC/hexadecane	26.05		21.04		11.47
DPhPC/buffer	47.35	10.89		11.47	

base model simulates two-phase fluid flow in a microfluidic T-junction in three dimensional space. The fluid interface is modelled by the level-set method,<sup>?</sup> which is notable for allowing droplets to break off. In order to speed up computation time, this model also utilizes a plane of symmetry to simulate only one half of the microfluidic channel. We modified the model with the density and viscosities of hexadecane and water, and the physical dimensions of the microfluidic devices used in this work. We then tuned the parameters of the simulation to ensure fast computation times, a stable fluid interface, and that a solution could be converged to by the solver through an iterative process using COMSOL LiveLink for MATLAB. We then derived a formula for the contact angle of a wetted wall within COMSOL from Young’s equation (see Supporting Information), which uses the contact angles for the oil and aqueous solutions obtained experimentally on PDMS in air. We also used literature data for other relevant contact angles and interfacial tension values. These data will change for other materials used for microfluidic device fabrication, such as polymethyl methacrylate (PMMA) or polycarbonate (PC), or in cases where droplets are formed in wells, rather than in flow as shown here. All interfacial tension values used are provided in Table 1.

The models were run in parallel on a Linux (v3.10) cluster operated by Compute Canada with a single compute node for each experimental condition and a time step resolution of  $1.25 \times 10^{-3}$  s and  $3.125 \times 10^{-4}$  s for the droplet length and contact angle sweep simulations respectively. The simulation was run over a time window of 0.05 s to 0.1 s depending on the number of droplets required. All models were run with an oil flow rate ( $v_{oil}$ ) of  $8.333 \mu\text{L min}^{-1}$

and an aqueous flow rate ( $v_{aq}$ ) of  $1.25 \mu\text{L min}^{-1}$ . These flow rates were chosen based on those that allowed stable droplet formation *in situ*, and the ratio of oil flow rate to water flow rate was kept the same for all experiments so as to not impact our findings. A visualisation of the results of a droplet length experiment can be seen in Figure 2A, where a droplet has formed in the channel and is indicated. Figure 2B shows the key dimensions for the model which will be referred to throughout this text.

### ***In silico* simulation of no lipid, lipid-in and lipid-out systems**

*In silico* models were prepared with equilibrium contact angle and interfacial tension data for three systems: hexadecane and water (no lipid), hexadecane and  $10 \text{ mg mL}^{-1}$  DPhPC in buffer (lipid-in), and  $10 \text{ mg mL}^{-1}$  DPhPC in hexadecane and buffer (lipid-out). The contact angles for each solution on PDMS in air were determined experimentally ( $39^\circ$  for hexadecane,  $114^\circ$  for water,  $23^\circ$  for DPhPC in hexadecane and  $70^\circ$  for DPhPC in buffer) and we then used the equations derived from the Young's equation (see Supporting Information) to calculate the contact angle of each droplet phase on PDMS surrounded by each continuous phase (i.e., no lipid, lipid-out, and lipid-in). Literature values for dynamic viscosity ( $\mu$ ) and density ( $\rho$ ) for hexadecane ( $\mu = 3.04 \text{ mPa}\cdot\text{s}$  and  $\rho = 0.770 \text{ g cm}^{-3}$ ),<sup>?</sup> and COMSOL material library values for water ( $\mu = 1.00 \text{ mPa}\cdot\text{s}$ ,  $\rho = 1.000 \text{ g cm}^{-3}$ ) were used. Changes to density for both phases with DPhPC dissolution were ignored, as the mass of DPhPC dissolved in a  $10 \text{ mg mL}^{-1}$  solution did not exceed 1.5% of the liquid mass, and very large (order of magnitude) changes to density are needed to make a significant difference in the process of droplet formation.<sup>?</sup> Similarly, given the low relative concentration of phospholipid, changes to viscosity were ignored as they were smaller than the doubling or halving of magnitude typically needed to measurably affect droplet formation.<sup>?</sup> The results of the simulations were post-processed using ImageJ (version 1.52D) to measure the length of the droplets, with channel width used as a known reference length ( $100 \mu\text{m}$ ) to calibrate the measurement tool.

## ***In situ* characterisation of droplets formed with and without lipid**

Microfluidic devices were run under the same conditions that were modelled *in silico*, as well as at two additional flow rates. The two additional flow rates were twice and four times higher than the original flow rate while maintaining the same flow rate ratio between the two fluids. To validate the *in silico* results we needed to ensure that the surface properties of PDMS were as close as possible to their initial state when making a comparison. For this reason, only the first 5 droplets formed during the run were used for validation of droplet length measurements. To collect footage of the first 5 droplets, flow on the aqueous pump was first reversed for 90s to draw the aqueous phase back inside the inlet tubing. Forward flow was then restored, ensuring that the aqueous phase would be flowing at the correct velocity when it once again reached the device and reached the T-junction. The high speed camera was triggered upon formation of the first droplets. Videos were captured at 200 fps. Measurements of droplet length were carried out in Phantom CineViewer 3.5.792.0 or using a simple Python script, using the channel width as a known reference length (100  $\mu\text{m}$ ) to calibrate the measurement in each case. A new microfluidic device was used for each condition to ensure a pristine surface prior to insertion of the fluids.

## **Statistical analysis of data**

Statistical analysis was performed to compare between *in silico* measurements and the initial droplets formed under each experimental condition. A three-level (for the three experimental conditions) one-way analysis of variance (ANOVA) was performed on the *in silico* droplet length and *in situ* droplet length data sets separately, to determine if phospholipid presence had a statistically significant effect on droplet length *in silico* and *in situ* (for the first 5 droplets only). A two-level (for *in situ* and *in silico*) one-way ANOVA was performed to compare each *in situ* droplet length population to its *in silico* counterpart collected under the same conditions, and determine if there was a statistically significant difference between predicted and actual droplet lengths. A two level (for *in situ* and *in silico*) one-way ANOVA

was also carried out to compare each lipid-containing *in situ* condition to the no lipid *in silico* condition, to establish if the addition of lipid made the droplet length measurably different from that predicted for a no lipid system. For all statistical analyses, the threshold for statistical significance was set at  $p < 0.05$ .

### ***In silico* sweep of observable contact angles**

To determine the relationship between on-device contact angle ( $\theta_{device}$ ) and the degree to which the fluid interface recedes following droplet formation ( $d_{recession}$ ), seven COMSOL models were prepared. Instead of calculating  $\theta_{device}$  using the derivation of the Young's equation shown in the Supporting Information, these seven models were each hard coded with a numerical contact angle. The chosen contact angles were evenly distributed over the range of  $120^\circ$  to  $180^\circ$ , encompassing the full range of values which had been previously determined with the equation. All models were run using the interfacial tension value for a hexadecane/water system ( $55.2 \text{ mN m}^{-1}$ )<sup>?</sup> for simplicity.

### ***In situ* characterisation of surface property changes over time**

Characterisation of surface property changes over time was carried out for no lipid, lipid-in and lipid-out at  $v_{oil}$  of  $8.333 \mu\text{L min}^{-1}$  and  $v_{aq}$  of  $1.250 \mu\text{L min}^{-1}$  *in situ*. To quantify surface property evolution, video footage was recorded with the high speed camera beginning when the first droplets formed, as described above. However, rather than collecting only the first 5 droplets, footage was collected for a prolonged period of up to 100 seconds or more unless device failure occurred earlier. A sample of at least 10  $d_{recession}$  values for each replicate was then measured with CineViewer.

# Results and discussion

## Determining the validity of the *in silico* model

We have designed an *in silico* (computational) model and, together with experimental (*in situ*) data, used it to better understand the effect that lipids have on the formation of droplets for the creation of DIBs at a microfluidic T-junction. The graphical representation of the *in silico* model and the key dimensions of the model and of the microfluidic device used for *in silico* and *in situ* data acquisition respectively can be found in Figure 2. In both cases, aqueous (buffer) droplets were formed in an oil (hexadecane) phase at a microfluidic T-junction, with the lipid (DPhPC) dosed in either of the two phases. Control data without lipids were also gathered.

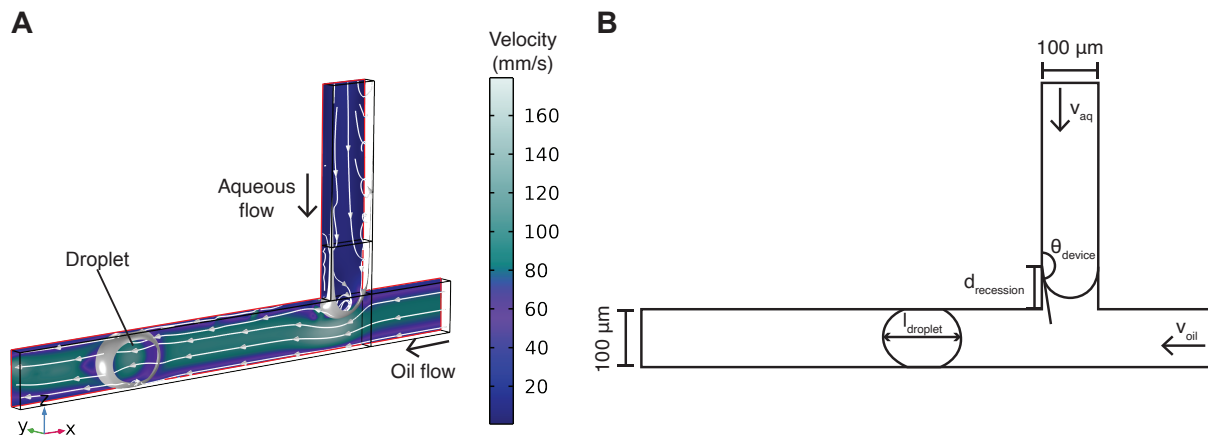


Figure 2: **Graphical representation of the *in silico* model and dimensions of the microfluidic device.** **A)** Three dimensional perspective rendering of the model in COMSOL Multiphysics, showing results for lipid-out droplet formation during droplet length experiments. The coloured velocity field slice is on the same plane as the plane of symmetry which is highlighted in red, and a single droplet can be seen travelling down the channel. Streamlines are shown with white arrows for direction, also showing convective mixing at the interface between the aqueous and oil phases. Black arrows denote the direction of flow for both the aqueous and oil phases within the microfluidic device. **B)** Key dimensions referred to throughout the text used to quantify characteristics of droplets formed both *in silico* and *in situ*, where  $v_{aq}$  and  $v_{oil}$  refer to the velocity of the aqueous and oil phases, respectively,  $\theta_{device}$  is the angle at which the fluid contacts the wall,  $d_{recession}$  is the distance receded by the fluid interface following droplet formation and  $l_{droplet}$  is the droplet length.

When developing an *in silico* model it is important to determine how well it mimics and hence predicts real-world situations. The validity of our *in silico* model was verified according to whether it accurately predicted droplet length under control (no lipid) conditions *in situ*. If the model satisfied this criterion, we could then attempt to use it to predict and explain the droplet lengths which would be observed for the other *in situ* (lipid-out, lipid-in) conditions. First, we determined whether the *in situ* and *in silico* droplet lengths were significantly different (two level ANOVA) for the no lipid condition. Then, to check whether the addition of lipid caused a change in droplet length *in silico*, we carried out a three way ANOVA between no lipid, lipid-out and lipid-in conditions.

Our data show that the *in silico* model we developed satisfies our proposed criterion for validity, as shown in Figure 4. We measured the length (as a proxy for volume) of a droplet following its formation at a T-junction both *in silico* and *in situ* with no lipid present in the system. The first column in Figure 3A shows representative images under the no lipid condition. We analysed the droplet length formed with no lipid in the system and two-level ANOVA between the *in silico* and *in situ* droplet lengths showed no statistically significant ( $p=0.38$ ) difference between them. Figure 3B shows these *in silico* (purple) and *in situ* (green) data for the no lipid condition.

We then changed the contact angle and interfacial tension values in our *in silico* model to match those of the conditions with lipids (i.e., lipid-in and lipid-out) with the aim of determining whether it was able to show the effect that lipids have on the droplet length. These simulations ignore mass transfer and adsorption effects to focus on modeling the effect of the surfactant on the interfacial tension and contact angle only. These data are shown in purple in the rest of the graph shown in Figure 3B. Three level ANOVA between the three *in silico* conditions revealed a statistically significant difference between the no lipid, lipid-out, and lipid-in conditions ( $p=7.4^{-6}$ ). Therefore, we conclude that the model does not include all of the physics required to predict the droplet length when lipids are added.

To understand the lack of change in droplet length upon addition of lipid, we remind the

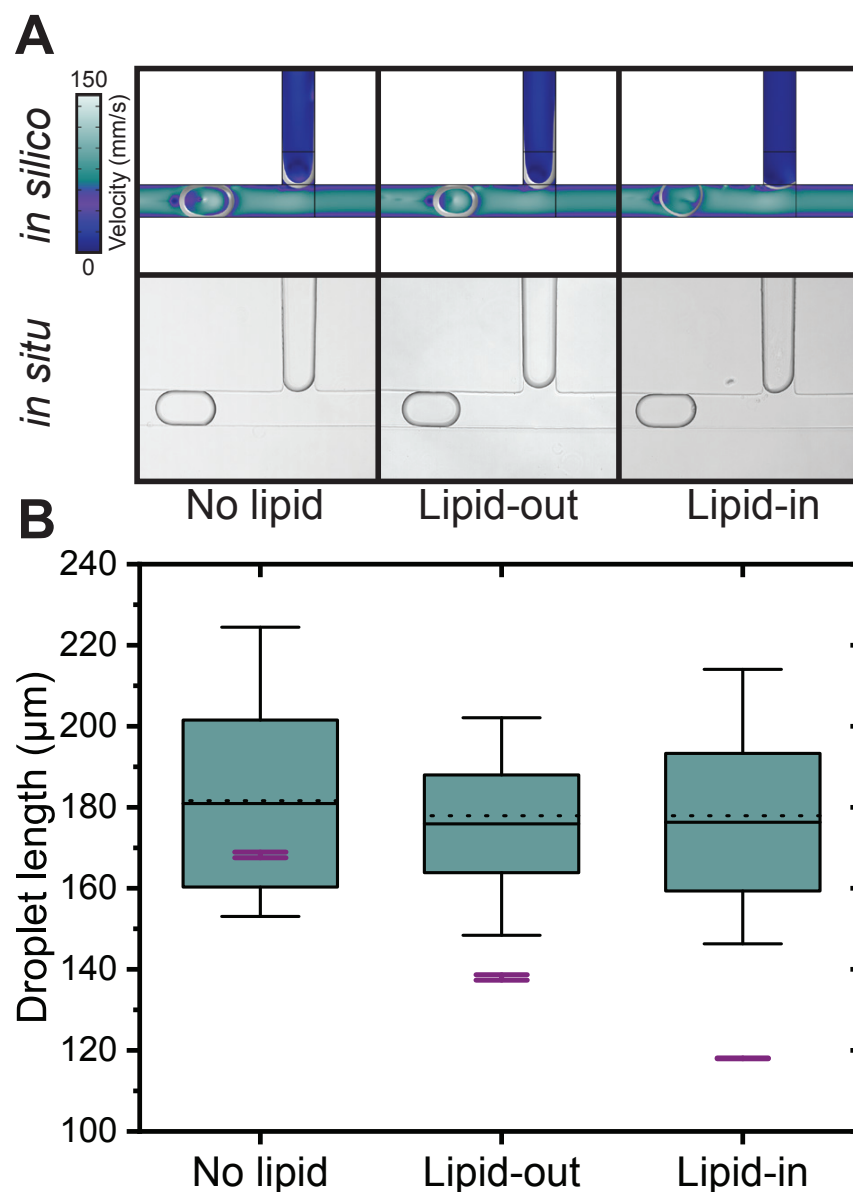


Figure 3: **Results of validation experiments.** **A)** Representative examples of droplets formed *in silico* (top) and *in situ* (bottom). The velocity scale bar applies to all *in silico* data. **B)** Green box and whisker plots show the distribution of droplet lengths observed for *in situ* data ( $n = 33$  for each) and purple mean and standard deviation plots show the predicted lengths ( $n = 2$  for each) for *in silico* data. Mean is shown on the box and whisker plot as a solid line, and median as a dotted line.

reader that this comparison was done using only the first 5 droplets. This means that it is possible that at early times the channels may still be equilibrating in one or more ways. For example, we see in Figure 3A that the contact angle *in situ* does not completely match the contact angle *in silico*. This is likely due to mass transfer effects, but could also be due in part to complexities related to defining a contact angle since we have not attempted to include contact angle hysteresis. However, because of this, we will also compare our results with measurements of thousands of droplets at later times in the following section.

## Determining the effect of phospholipids on droplet formation *in situ*

The reduced droplet size observed for lipid containing solutions *in silico* is expected due to their reduced interfacial tensions:  $21.04 \text{ mN m}^{-1}$  for lipid-out and  $10.89 \text{ mN m}^{-1}$  for lipid-in, compared to  $55.2 \text{ mN m}^{-1}$  for no lipid.<sup>??</sup> Another factor that is known to affect droplet length is the contact angle, with higher contact angles resulting in smaller droplets.<sup>?</sup> This contact angle effect is consistent with the decrease in droplet length observed in the lipid-out conditions, where  $\theta_{device}$  increased from  $157^\circ$  for no lipid to  $180^\circ$  for lipid-out. However, lipid-in conditions exhibited the smallest droplet length, despite the contact angle being smaller at  $121^\circ$ . Hence, the greatest factor affecting droplet length *in silico* appears to be the interfacial tension, as otherwise the contact angle decrease seen with the lipid-in conditions would very likely lead to droplets being larger than observed, as the effects of contact angle and interfacial tension on droplet size are working in opposition to each other.<sup>??</sup>

Carrying out two-level statistical comparison between the *in situ*, lipid containing conditions, and the *in silico*, no lipid condition, there was no statistically significant difference observed for either lipid-out ( $p=0.35$ ) or lipid-in ( $p=0.48$ ). This demonstrates that, at least for the first 5 droplets, both lipid-out and lipid-in systems *in situ* behave indistinguishably from the predicted behaviour of a system containing no lipid. These findings are surprising for a microfluidic system, as it is known that stable DIBs can be formed on a microfluidic de-

vice orders of magnitude faster than in bulk solution,<sup>?</sup> suggesting that the assembly of lipid at the fluid interface should also be considerably faster than those determined by the pendant drop method.<sup>?</sup> However, it is important to note that we are studying how droplet formation occurs when phospholipids are present. DIBs will only form if the droplets come together slowly enough once they are properly covered with a phospholipid monolayer, otherwise droplets will merge. This also highlights the possible pitfalls in extrapolating computational data to the real world, as literature *in silico* determination of the relationship between interfacial tension and droplet size may be misleading when predicting a corresponding droplet size upon addition of surfactant.

However, we can also look beyond the first 5 droplets to see what happens at longer times. Therefore, to gain more insight into the dynamics of equilibration we also measured the average droplet size for thousands of droplets during continuous operation of the microfluidic device for three different flow rates at each of the three lipid conditions. The droplet lengths measured for each case are plotted in Figure 4 as a function of the Capillary number,  $Ca$ , defined as:

$$Ca = \frac{\eta Q}{A\gamma}. \quad (1)$$

Here  $\eta$  is the viscosity and  $Q$  is the volumetric flow rate of the continuous phase (oil),  $A$  is the cross-sectional area of the channel where the droplets are formed, and  $\gamma$  is the interfacial tension. In each case, the equilibrium value of  $\gamma$  was used to generate the plot.

Figure 4 shows several interesting results. First, we see that the average droplet length for the three lipid conditions are still approximately the same at the lowest flow rate (the lowest Capillary number for each data set), though they are larger than the first 5 droplets. The increased size at later times shows that indeed there is some kind of equilibration that is not yet complete for the first 5 droplets. However, it also highlights the importance of using appropriate non-dimensionalization when comparing conditions. Specifically, if one only compared the droplet length for each of the three lipid conditions at the lowest flow rate, one might conclude that adding lipid makes no difference. However, the systems can only be

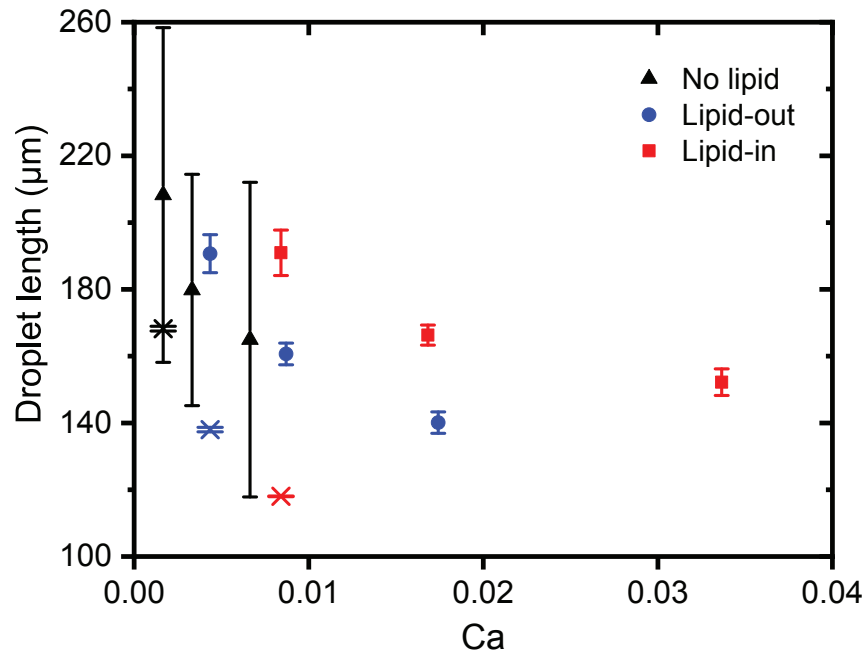


Figure 4: **Results of droplet length experiments.** Mean and standard deviation of the droplet length as a function of Capillary number,  $Ca$  ( $118 \leq n \leq 10931$  for each condition). The “x” symbols correspond to the *in silico* results with the color indicating the condition it was intended to match. Note that for each lipid condition *it situ* the three different values of the Capillary number correspond to three different flow rates, while for the *in silico* condition, the three Capillary numbers correspond to different values of the interfacial tension at the lowest of the three flow rates.

called hydrodynamically equivalent when they are operated at the same Capillary number<sup>?</sup> and so should only be expected to have the same droplet length if the Capillary number (and other relevant dimensionless quantities like viscosity ratio, flow rate ratio, geometric aspect ratios, etc.) are the same.

In line with the previous point, another result that we see in Figure 4 is that at the same Capillary number, the mean droplet size for each condition is quite different. This proves that adding lipid changes the droplet formation process and that adding lipid to the droplet phase (lipid-in) is different from adding it to the continuous phase (lipid-out). The reasons for this difference are discussed in more detail in the next section. A final result that we wish to point out in Figure 4 is that standard deviation in the droplet length for the no-lipid case is much larger than the other conditions. This is not unexpected since droplet formation is known to be disordered for a system without surfactant, and the formation process is irregular.<sup>?</sup>

## **Determining the effect of phospholipids on long-term microfluidic device operation**

In addition to playing a role during droplet formation, we have previously shown that surfactants in microfluidic devices also change the surface properties of the rest of the device.<sup>?</sup> Having established that lipids alter the droplet formation to affect droplet length, we then examined the effect of lipids on the wetting properties of the microfluidic device. In order to examine whether there are any changes to the surface properties of the microfluidic device during operation *in situ*, a relationship between contact angle, as a means to quantify wetting characteristics, and a parameter that can be seen visually on a microscope needed to be established. One such variable is the recession distance ( $d_{recession}$ ), which is the distance that the aqueous fluid recedes into the inlet channel after the formation of a droplet (Figure 2B). Note that there is no backflow in the device and this recession distance is simply a reflection of the location where the droplet broke away from the upstream fluid.

We have observed experimentally that as devices develop poor wetting properties, the distance that the fluid interface recedes following droplet formation grows shorter. Moreover, we have observed that shortly after  $d_{recession}$  reaches zero, the aqueous fluid interface begins to move further into and down the channel, a critical step in the transition to the dripping droplet failure mode (Figure 1).<sup>?</sup> To test whether  $d_{recession}$  was a suitable visual reporter parameter for the change in device surface properties, we used our *in silico* model to perform a single-parameter, parametric sweep of device contact angles ( $\theta_{device}$ ) over the range of 120° to 180°, and ran each of the models over the window of time needed for three droplets to form, to confirm whether a clear relationship between the  $\theta_{device}$  and  $d_{recession}$  exists. This contact angle range was chosen to accommodate the entire range of contact angles seen *in silico* during the initial model validation.

While we readily acknowledge the limitations that we have already identified in the *in silico* model, precedent exists for using such an idealised model of droplet formation, as previous computational work relating droplet size to interfacial tension typically assumes that interfacial tension is a fundamental property of the fluid system, rather than a time-dependent process induced by a surfactant.<sup>????</sup> More specifically, prior work with the natural phospholipids found in soy lecithin shows the inability of solutions containing soy lecithin to form droplets lipid-out at a Y-junction, while Span 80 containing solutions did, which was explained by the poor mobility of lecithin in hexadecane, and therefore a slow drop in interfacial tension relative to Span 80.<sup>?</sup> Therefore, the *in silico* model was used as a qualitative check of our hypothesis that  $d_{recession}$  is correlated to  $\theta_{device}$ .

As shown in Figure 5 our *in silico* model shows a clear dependence of  $d_{recession}$  on  $\theta_{device}$ . This figure shows both the raw data for  $d_{recession}$  measured at each  $\theta_{device}$ , as well as an empirical fitted curve. A non-linear, positive relationship exists between  $\theta_{device}$  and  $d_{recession}$  over this range, showing that even under simplified conditions,  $d_{recession}$  is a suitable means of indicating changes in contact angle visually on microscopy images for subsequent *in situ* experiments. With this quantitative relationship between  $d_{recession}$  and  $\theta_{device}$  established,

we have a means of characterising the surface properties of a microfluidic device during its operation and we can hence examine the effect of lipids on surface property evolution over time.

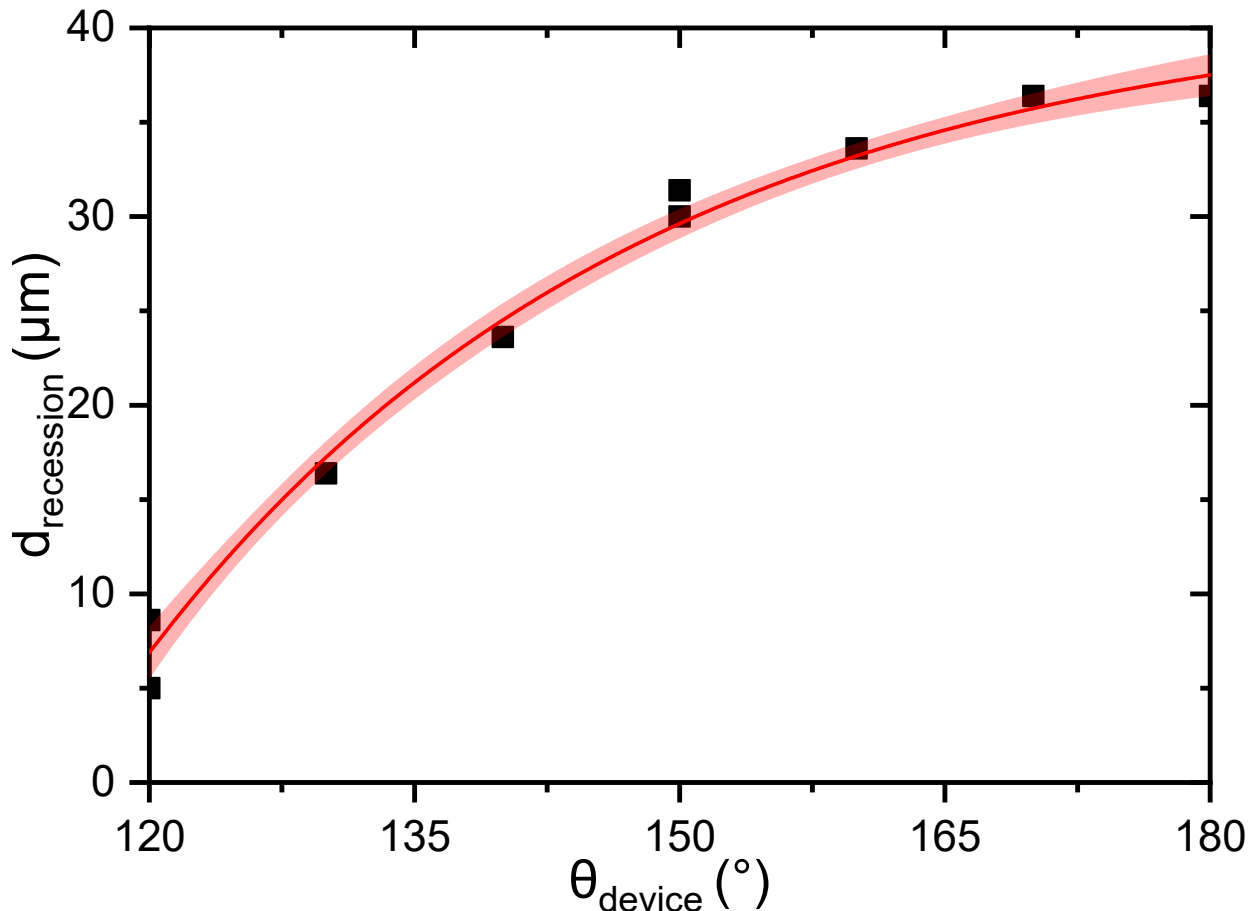


Figure 5: *In silico* relationship between contact angle and  $d_{recession}$ . These *in silico* data show the relationship between the contact angle ( $\theta_{device}$ ) on the device and the recession distance ( $d_{recession}$ ) of the fluid interface following droplet formation. Raw data ( $n = 3$  for each) is shown in black. Curve fit and 95% confidence bands are shown in red. The curve is fitted to an asymptotic equation of the form  $y = a - bc^x$  and has  $R^2 = 0.99$ .

To determine the effect of DPhPC on device surface properties, video footage of the microfluidic T-junction was collected from the point when water first reached the T-junction, until device failure. Device failure was defined to occur when when droplet formation ceased due to co-flow or the formation of plugs, whichever was first. The results of measuring  $d_{recession}$  for the first 100 s (or until device failure) are shown in Figure 6. This figure shows

quantitatively that  $d_{recession}$  decreases over time *in situ* for droplets created with no lipids (black squares), lipid-out (red circles) or lipid-in (blue triangles). This, in turn, implies a decrease in the contact angle, and an increase in the ability of the water to wet the channel, as time progresses.

In Figure 6 we also show images just after a droplet pinch-off event at the start of the flow (first row of images) and just after the point when  $d_{recession}$  is no longer visible (second row of images). This is clear visual confirmation that the wetting properties of the channel are changing over time and in each of the images an arrow shows the approximate location of the contact line where the droplet phase is still adhering to the wall. The effect is even more pronounced at later times as shown in the third row of images in Figure 6. At much later times we see that the contact line where the wetted region ends has progressed farther down into that channel forcing droplet breakup to occur further down the channel, resulting in transition to the dripping regime and eventually the co-flow regime.

When comparing the three different lipid conditions at later times, we see that in the lipid-out case the wetted region has propagated only a short distance into the channel even at very long times. The lipid-in case however has allowed the wetted region to propagate about halfway down the visible portion of the channel in approximately the same amount of time, resulting in the dripping failure mode. Finally, in the no lipid case, the wetted region has quickly propagated beyond the visible portion of the channel resulting in complete device failure.

Surfactants are known to coat the walls of PDMS based microfluidic devices during their operation, contributing to their equilibrium surface properties.<sup>?</sup> It is also generally assumed that a surfactant dosed in the aqueous phase of water-in-oil droplets has no effect on the surface properties of the microfluidic device. However, it is common in the field of microfluidics to “prime” the channels in the microfluidic device by flowing only the lipid-out oil phase through the device prior to droplet formation, though it is not clear whether it is the oil or the surfactant (or both) that is affecting the surface characteristics during this

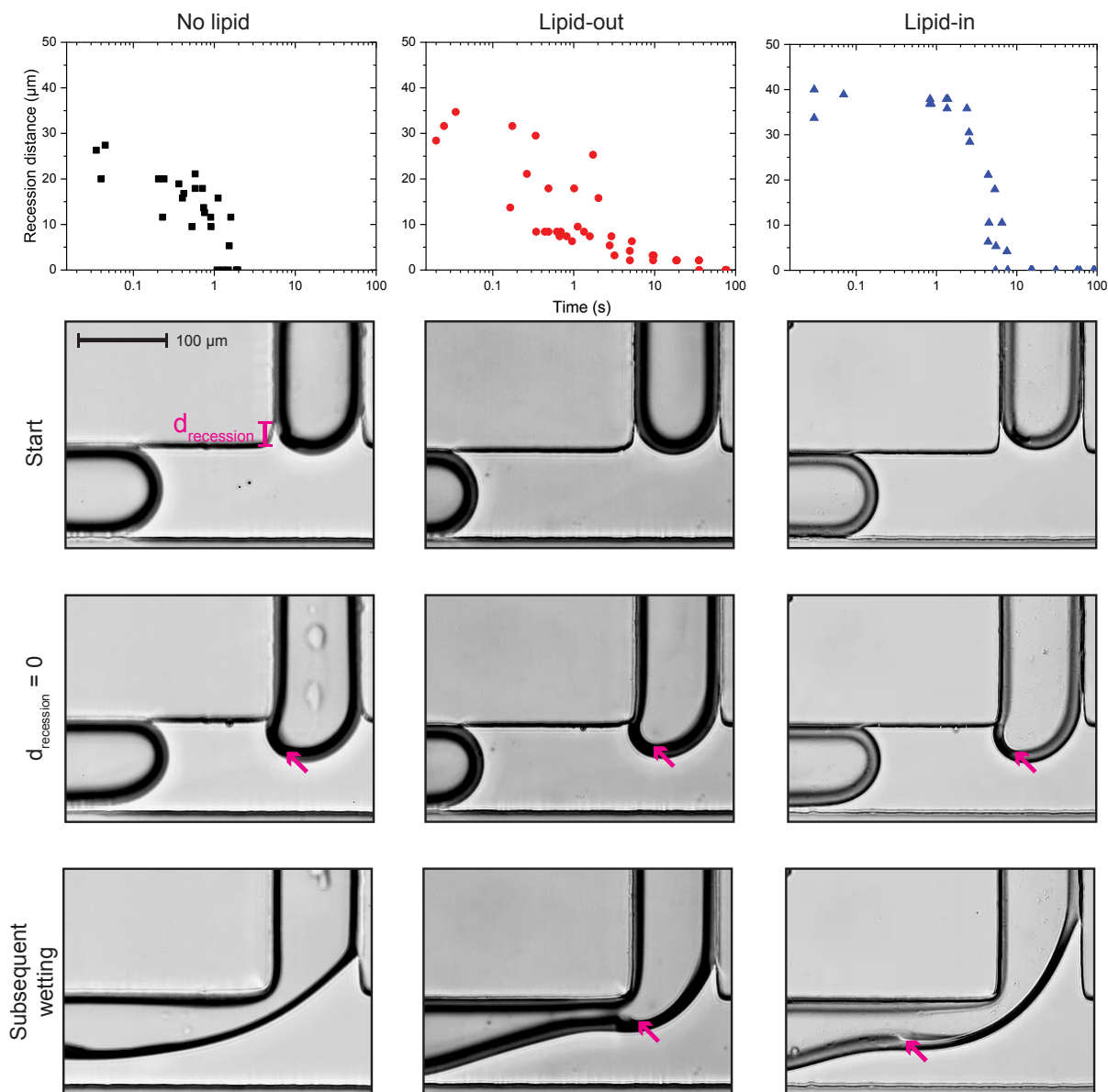


Figure 6: **The effect of lipid presence on device longevity.** Surface property evolution is quantified as *in situ* decrease of recession distance. No lipid is shown with black squares, lipid-out with red circles, and lipid-in with blue triangles. Note that in the case of no lipid, complete failure of droplet formation occurred at  $t = 1$  s and hence recession distance was not quantifiable after this point.  $N = 3$  for each condition and all data are plotted to aid trend visualisation. The first row of images are taken just after droplet formation at the start of the experiment, the second row of images is taken when  $d_{recession}$  is no longer visible, which over time becomes much more pronounced, as shown in the third row of images. Arrows denote the location of the wetting contact line. The scale bar applies to all images.

process. Here we wanted to study the effect that the presence of lipids has on the longevity of the device. Our data provide the first *in situ* quantification of the different rates of surface property changes when phospholipids are used in a PDMS microfluidic device.

The data in Figure 6 show that the addition of lipid clearly affects the device longevity, whether it dosed in the oil phase or the aqueous phase. Where no lipid is present droplet formation ceases to be possible within 1 s of device usage. When lipid is added lipid-out there is a gradual decrease in device performance over time, as signified by the drop in the recession distance. This means that droplet formation ceases to occur cleanly at the T-junction and begins to occur further into the channel over the course of 100 s. When the lipid is added lipid-in, this process occurs much more suddenly at around 1 s after initiation of droplet formation. These data show that the surfactant-like behaviour of lipids in microfluidic devices is complicated.

We measured the contact angle of oil on PDMS to be  $39^\circ$ , which decreases to  $23^\circ$  upon the addition of lipid. Likewise, we measured the contact angle of the aqueous phase on PDMS to be  $114^\circ$ , which decreases to  $70^\circ$  upon the addition of lipid. This suggests that the lipid behaviour is changing based on its preference for interaction with the oil phase or with the surface of the PDMS. The decrease in contact angle upon addition of the lipid to the oil phase suggests that the lipid enhances the wetting of the oil to the PDMS surface by making the surface more lipophilic, and hence that the lipid molecules arrange themselves tail out on the channel surface. Likewise, the decrease in contact angle upon addition of the lipid to the aqueous phase suggests that when droplets are in contact with the channel walls, the lipid makes the surface of the PDMS more hydrophilic, and hence that the presence of droplets encourages the lipid molecules to arrange themselves headgroup out on the channel surface.

We therefore rationalize our findings as follows. In the lipid-out case, the gradual decrease in the recession distance indicates that the surface of the channel is becoming more hydrophilic over time as more droplets are created, which agrees with our prior work showing

that droplets effectively strip the surfactant from the channel surface causing wetting of the aqueous phase.<sup>?</sup> After 100s of device operation, we can still form droplets but these are created further down the channel. In the lipid-in case, initially the device behaviour follows the same trend as with the no-lipid case, but after about 10s mass transfer of the lipid from the droplet to the channel wall makes the walls even more hydrophilic than in the lipid-out case.

## Conclusions

Here we have provided the first detailed characterisation of the behaviour of phospholipids in droplet microfluidic devices for DIB formation, and how this affects the design of the microfluidic device. With our COMSOL *in silico* model and *in situ* experimental data, we have found that migration of phospholipids to or from the PDMS surface occurs over the course of device operation. This causes droplet formation to be strongly affected by the presence of lipids. We also found a relationship between contact angle and the visually distinguishable parameter of recession distance through use of our *in silico* model. By quantifying recession distance *in situ*, we carried out the first characterisation of the evolution of surface properties during operation of PDMS microfluidic devices in the presence of phospholipids. This understanding of the fundamental role of phospholipids as surfactants in droplet systems will enable more targeted designs of microfluidic platforms, where geometric features can be adapted to suit the behaviour of phospholipids in these systems.

## Acknowledgements

The authors thank Dr. Djilali for use of his equipment for carrying out interfacial tension measurements. This research was enabled through computational facilities provided by WestGrid and Compute Canada. COMSOL and COMSOL Multiphysics are registered trademarks of COMSOL AB. The author is not affiliated with COMSOL AB and COMSOL

AB has not authorized, sponsored, or approved this work.

Dr Elvira's position is funded through the Canada Research Chair program and the Michael Smith Foundation for Health Research Scholar program in partnership with the Pacific Alzheimer Research Foundation. This research was funded through Dr Elvira's Natural Sciences and Engineering Research Council of Canada (NSERC) Discovery grant. Her laboratory was equipped using funding from the Canada Foundation for Innovation John R. Evans Leaders Fund, the British Columbia Knowledge Development Fund the NSERC Research Tools and Instruments program.

## Contributions

RGR modified the COMSOL library microfluidic model to add the density and viscosities of hexadecane and water, and the physical dimensions of the microfluidic device, and tuned the parameters to ensure fast computation times and a stable fluid interface. EBS further adapted the COMSOL model to incorporate experimental contact angle and interfacial tension measurements using the derived equation, modified it to report additional values, designed and carried out all *in situ* and *in silico* experiments shown here, analysed the data and wrote the original draft of the manuscript. KAH and GL carried out the contact angle measurements. SF gathered the interfacial tension data with the help of JMF. JMF provided expertise in surface properties and contact angles, as well as building the interfacial tension instrument and writing the custom software required for data analysis. KSE and JMF reviewed and edited the manuscript, and KSE supervised EBS, RGR and SF. All authors approved the final version of the manuscript.

## Supplementary Material

Derivation of the contact angle from Young's equation.